Applied Catalysis B: Environmental 168-169 (2015) 363–369

Contents lists available at ScienceDirect

Applied Catalysis B: Environmental

journal homepage: www.elsevier.com/locate/apcatb

Silica nanoparticles assisted photodegradation of acridine orange in aqueous suspensions

Roberta Selvaggi [a], Luigi Tarpani [a], Alessia Santuari [a], Stefano Giovagnoli [b], Loredana Latterini [a,*]

[a] Department of Chemistry, Biology and Biotechnology, University of Perugia, Via Elce di Sotto 8, 06123 Perugia, Italy
[b] Department of Pharmaceutical Sciences, University of Perugia, Via del Liceo 1, 06123 Perugia, Italy

ARTICLE INFO

Article history:
Received 13 August 2014
Received in revised form
15 December 2014
Accepted 31 December 2014
Available online 3 January 2015

Keywords:
Photocatalysis
Silica nanoparticles
Silica surface modification
Cationic heterocyclic dye
Acridine orange zinc chloride double salt

ABSTRACT

Silica nanostructured materials are often used as catalyst support but their catalytic role has not been deeply investigated yet. In the present study, the photocatalytic degradation of acridine orange zinc chloride double salt (AO) has been studied using silica nanoparticles (NPs) as catalysts. NPs of different size (55 and 146 nm) were prepared by a sol–gel procedure and their surface was modified with amino groups to investigate the role of the chemical groups linked to the silica surface on the dye degradation. The silica nanomaterials were fully characterized by use of transmission electron microscopy (TEM), zeta potential measurements and UV–vis spectrophotometric methods.

The photodegradation experiments were carried out irradiating at 313 or 490 nm for 50 min the aqueous samples containing the dye and the silica NPs of 55 or 146 nm in diameter. The photocatalytic degradation of the dye was determined from the decrease of its fluorescence intensity. AO fluorescence intensity did not change when bare SiO_2 beads were used as catalysts, whereas an efficient decoloration (up to 58%) was achieved with amino functionalized NPs, with a photodegradation rate constant value of 0.136 m^{-1}. The data collected from the degradation experiments demonstrated that the functional groups on the silica surface have a fundamental role in the efficiency of the degradation processes.

1. Introduction

Wastewater discharged by dye manufacturing and textile finishing industries has become an environmental concern since it contains relevant concentrations of synthetic organic dyes, which are characterized by very high COD and TOC values as well as high colouring capacity [1].

Dye wastewater discharged from the textile industry can damage water resources. The presence of even small amounts of dye is highly visible and affects the optical properties of the water and consequently the photosynthetic activity of aquatic organisms and the solubility of gases. Besides, the textile dyes might have toxic and potentially carcinogenic effects [2].

Synthetic dyes are prepared to ensure high stability to light, temperature, acids, bases, oxidizing agents and microbial agents, as these are the desired properties of the dyed clothes. Therefore, it is difficult to treat wastewater and to remove dyes using conventional techniques. Clean and cost-effective technologies for the degradation of organic pollutants have become an important industrial concern.

In the last decades, based on the development of nanostructured materials and the understanding of their optical and electronic properties, nanomaterial-assisted photocatalytic methods have been proposed. It has been shown that specific interactions occur in hybrid colloidal systems at the interface between the semiconductor nanocrystals and organic moieties adsorbed/coordinated on the semiconductor surface, and these interactions modify the photochemical/photophysical behaviour of the colloidal system [3]. In particular, much attention has been paid to the study of titanium and zinc oxide nanostructures and their impact on the photocatalytic degradation of organic pollutants [4–7]. These materials show important electronic properties that have attracted the interest of industry and researchers particularly aimed at the cost-effectiveness optimization of preparation methods [8]. Among others, titania and zinc oxide materials have wide band gaps (3.0–3.2 eV), which confer strong absorption capacity over a large portion of the UV solar spectrum. The investigation of the semiconductor properties of such materials improved

* Corresponding author. Tel.: +39 75 5855636; fax: +39 75 5855598.
E-mail address: loredana.latterini@unipg.it (L. Latterini).

http://dx.doi.org/10.1016/j.apcatb.2014.12.051
0926-3373/

understanding and description of the underlying photocatalytic mechanisms [9–16]. The principle of the semiconductor photocatalytic reaction is widely accepted [17]. Upon absorption of photons with energy larger than the band gap of the semiconductor, electrons are excited from the valence band to the conduction band, creating electron–hole pairs. These charge carriers migrate to the surface and react with water and oxygen generating radicals or intermediate species such as $OH^{\bullet}$, $O_2^{\bullet -}$, and/or O_2, which decompose the organic chemicals adsorbed on the surface of the semiconductors [18].

Different engineering approaches have also been developed to narrow the material band gap and improve solar light absorption ([19] and references there in). One of the most widely investigated strategies is based on dye absorption. Under visible light illumination, the adsorbed dye is excited and subsequently electron injection or transfers (even through intermediate species) assisted by the semiconductor can occur. These processes lead to the formation of reactive radical species, such as hydroxyl radicals, able to degrade the molecules adsorbed on the particle surface.

Titanium dioxide, especially the anatase-phase nano-titania [20], is the photocatalyst with the best photocatalytic performances, but its use is too expensive for large scale water treatment. Different semiconductors, such as SnO_2, ZrO_2, CdS and ZnO, have been tested as photocatalysts for the degradation of dyes [15–17,21–25]. In particular, Kansal and co-workers obtained methyl orange and rhodamine 6G aqueous solution photocatalytic decoloration efficiencies above 90% using ZnO [26].

Silica has a very wide band gap (nominally 8.9 eV) making this material transparent to vis radiations. For these properties, it has been used to entrap dyes and drugs in order to improve stability as well as delivery [27–29]. However, the presence of structural defects alongside the reduced crystallinity can decrease the band gap energy or enhance the material photoactivation capacities in the UV-region [30]. Silica has a quite reactive surface due to the presence of silanol groups, capable of adsorbing organic and inorganic species and this property can be enhanced when silica is shaped as colloidal particles [30–32]. Silica nanomaterials exhibit measurable photocatalytic activity under UV irradiation [30–34], lower costs as compared to TiO_2 and ZnO and much lower environmental impact.

In this regard, silica nano-phases have been synthesized and employed to oxidize dyes. Badr and Mahmoud used silica nanoparticles and silica coated silver and gold NPs as photocatalysts for the degradation of methyl orange dye under xenon lamp excitation [35]. They observed that silica coated Ag and Au NPs show enhanced photocatalytic degradation compared to silica NPs and this is due to the reduction of the electron–hole recombination process, which favours the formation of $OH^{\bullet}$ radicals.

In the present study, in order to explore the photocatalytic properties of silica colloids, the degradation efficiency of acridine orange zinc chloride double salt (AO) is determined in the presence of silica NPs. NPs of different size are prepared by a sol–gel method [36–38], characterized [27–29] and the effect of surface chemistry on the dye photodegradation is evaluated upon surface functionalization with amino groups [39–41]. The photoactivity of the samples is determined and compared by monitoring the fluorescence intensity decrease of AO after UV or vis monochromatic irradiation.

2. Materials and methods

2.1. Materials

Hexanol, cyclohexanol, Triton X-100, 3-aminopropyltriethoxysilane (APTES), Acridine Orange hemi (zinc chloride) salt (AO), acetone and aqueous ammonia solution (28–30% NH_3 basis) were purchased from Sigma–Aldrich (Sigma–Aldrich, St. Louis, MO, USA) and used without further purification. Tetraethoxysilane (TEOS) and ethanol were obtained from Fluka (Milwaikee, WI, USA). Analytical grade water was used for the preparation of the solutions.

2.2. Preparation of the photocatalysts

2.2.1. Preparation of silica nanoparticles through the microemulsion method

The NPs were prepared using a microemulsion method [37] in order to better control the growth process. The W/O microemulsion was prepared by mixing cyclohexane (75 mL), TX-100 (17.7 mL), hexanol (18 ml) and water (5.4 mL) under vigorous stirring. Then the hydrolysis and condensation reaction was initiated by adding 1 mL of TEOS and 0.7 mL of ammonia solution (28–30%) to the microemulsion and stirring for 24 h. The NPs were precipitated with acetone (40 ml), followed by centrifugation and washing with ethanol and water several times to remove the residual surfactant. Then the NPs (SNP1 sample) were dried in a water bath at 80 °C.

2.2.2. Preparation of silica nanoparticles through the Stöber method

The NPs were prepared using the method developed by Stöber [38]. 0.5 mL of water, 23 mL of ethanol, 0.8 mL of ammonia solution (28–30%) and 1 mL of TEOS were stirred for 24 h. After the reaction was completed, the NPs (SNP2 sample) were centrifuged, washed three times with ethanol and dried in a water bath at 80 °C.

2.2.3. Preparation of amine-functionalized silica nanoparticles

To functionalize the surface of silica NPs, APTES was dissolved in an ethanol:distilled water mixture (10:1) upon stirring for 6 h. The silica NPs (SNP1 or SNP2) were then added into the mixture and stirred at room temperature for 24 h. The sample was separated by centrifugation and washed twice with ethanol and once with water to remove the possible un-grafted APTES. The resulting powder was dried at room temperature. The functionalization of 1 mg of SNP1 or SNP2 was achieved using 561 μL and 1.48 mL of the ethanol:water:APTES mixture (10:1:1) [39].

2.3. Photocatalyst characterization

The morphology of SNP1 and SNP2 samples was investigated by transmission electron microscopy (TEM) using a Philips model 208 microscope working at 80 kV of beam acceleration.

The average sizes of NPs were measured by statistical analysis of TEM images using ImageJ software (National Institutes of Health, USA). The particle size data were based on the image analysis of more than 300 particles.

The zeta-potential data of NPs in water and ethanol suspensions (SNP1, SNP2, SNP1-APTES, SNP2-APTES) were determined by NICOMP 380 ZLS equipped with a HeNe Laser source at 632.8 nm (Particle Sizing System, Inc., Santa Barbara, CA, USA).

2.4. UV–vis absorption and fluorescence spectra of photocatalyst suspensions and dye solutions

Absorption spectra of the solid samples were recorded by a Cary 4000 (Varian Inc., Palo Alto, California, USA) spectrophotometer, equipped with a 150 mm integration sphere and a barium sulphate tablet as reference. The spectra were processed with the Kubelka–Munk equation in order to make possible the comparison.

Absorption spectra of the colloidal suspensions of the silica NPs and the dye were recorded with a PerkinElmer Lambda 800 spectrophotometer (Massachusetts, USA)

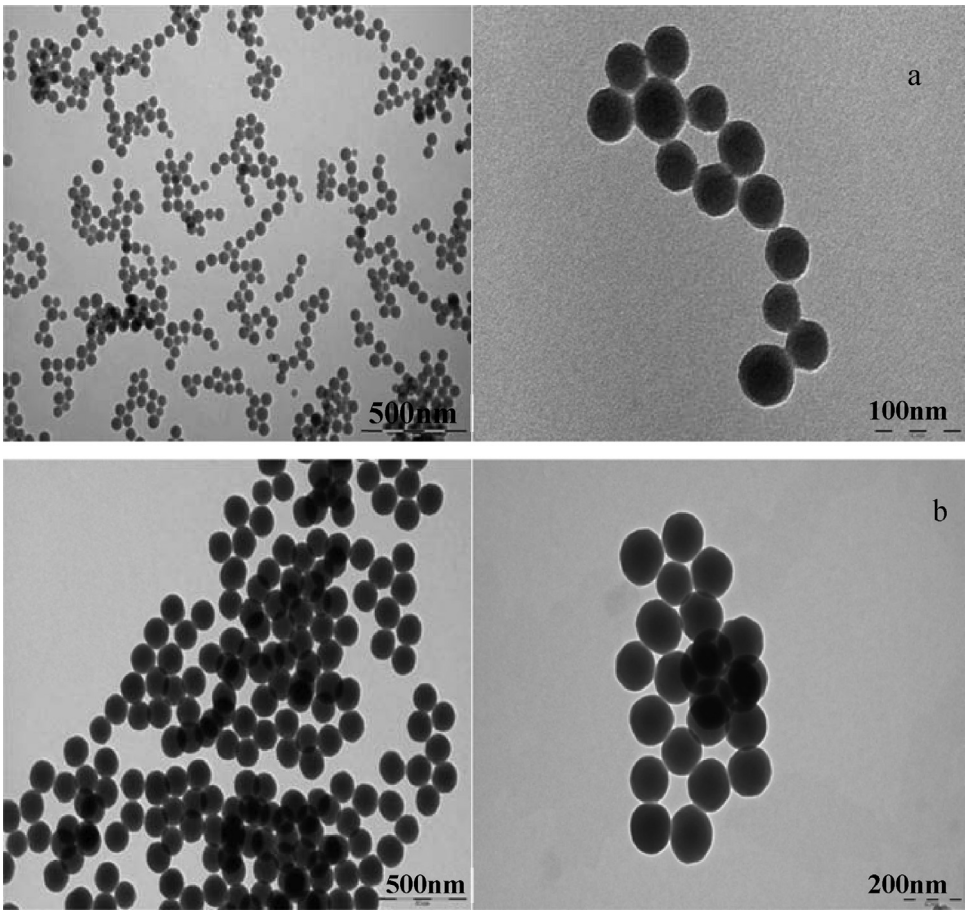

Fig. 1. TEM images of silica NPs: (a) SNP1; (b) SNP2.

A Fluorolog-2, model F112AI (Spex Industries Inc., Edison, NJ, USA) spectrofluorimeter was used to record fluorescence spectra of the dye in aqueous suspensions, using a front face configuration between the excitation and the emission light.

2.5. Irradiation experiments

Steady state irradiation experiments were performed using a 150 W Xenon lamp as light source and selecting the excitation wavelength (313 and 490 nm) by a monochromator. In order to monitor the effect of silica NPs on the photodegradation of AO, the photocatalyst (10 mg) was added to 3 ml of the aqueous solution of the dye (1×10^{-5} M); the resulting suspensions were irradiated for up to 50 min with UV or vis light. The aqueous suspension was magnetically stirred throughout the experiment. The progress of the degradation of dye was monitored recording the intensity of fluorescence emission at 530 nm (λ_{ex} = 490 nm).

3. Results

3.1. Morphologic characterization of the photocatalysts

3.1.1. Transmission electron microscopy (TEM)

The morphology of silica NPs (SNP1 and SNP2) is examined by TEM. The TEM images (Fig. 1) reveal that particles are spherical in shape and a good dispersion has been achieved through the used preparation conditions. The size distribution analysis (Fig. 2) enables to determine an average size of 55 ± 4 nm and 147 ± 6 nm for SNP1 and SNP2, respectively. Functionalization with 3-aminopropyltriethoxysilane (APTES) to obtain SNP1-APTES and SNP2-APTES does not alter the shape and size distribution of the particles.

3.1.2. Zeta potential measurement

Measurements of zeta potential are an important tool to evaluate surface charge distribution and the stability of the nanoparticle dispersions.

The zeta potential of SNP1, SNP2, SNP1-APTES, SNP2-APTES in water and ethanol are listed in Table 1. SNP1 and SNP2 particles show a negative surface potential ranging from −20 to −38 mV due to the presence of deprotonated silanol groups regardless the solvent in which the NPs are dissolved. However, silica samples that were modified on the surface with amino silanes (SPN1-APTES and SNP2-APTES) have a less negative to positive surface potential confirming that the surface functionalization with amine groups confers a positive contribution to the surface charge.

The data in Table 1 show that in this case the absolute zeta potential values depend on the solvent, ranging from −18 to +14 mV. In ethanol solutions, the NPs, with the exception of SNP2, show zeta potential values less negative than in water, likely due to a lower degree of dissociation of surface silanol groups in ethanol [42]. Moreover, SNP1 has a zeta potential value less negative than SNP2 in ethanol. This behaviour can be explained considering the effect of particle diameter on surface silanol structure. Kamiya et al. [43] have reported that in silica particles with diameters exceeding 60 nm most of the silanol groups are hydrogen-bonded silanol groups and in addition the hydrogen bond between O and H atoms promotes polarization in the other O—H groups. On the other hand, they observed that in case of particles with diameters smaller than 30 nm, the amount of isolated silanol groups increases, due

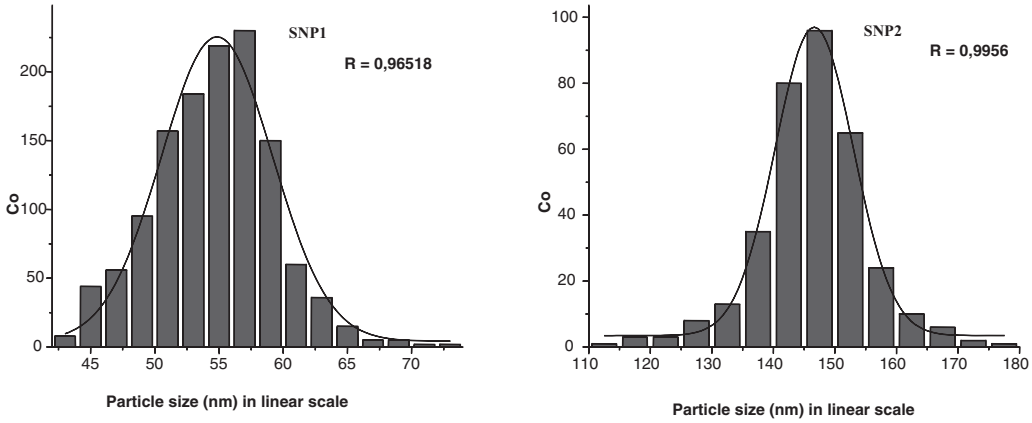

Fig. 2. Size histograms obtained by the statistical analysis of TEM images for SNP1 and SNP2 samples.

Table 1
Zeta-potential values of silica nanoparticle suspensions.

Catalyst	Z (mV) In EtOH	Z (mV) In H_2O
SNP1	−20 mV ± 5 mV	−37 mV ± 4 mV
SNP1-APTES	+5 mV ± 5 mV	−4 mV ± 3 mV
SNP2	−38 mV ± 5mV	−38 mV ± 5 mV
SNP2-APTES	+14 mV ± 5 mV	−18 mV ± 3 mV

to the large particles curvature; thus the polarization of isolated silanol groups is lower than that of the hydrogen bonded silanol groups.

Since SNP1 particles have a mean diameter below 60 nm, it is reasonable to expect that the amount of isolated silanol groups in SNP1 is higher than in SNP2, thus reducing the degree of polarization of O—H groups, resulting in a less negative zeta-potential value in SNP1 compared to SNP2.

3.2. Spectral characterization

Fig. 3 displays the UV–visible spectra of solid and aqueous suspension of silica NPs. The UV–vis absorption spectra of silica NPs in the powder form show a band-edge shape (maximum of the absorption band centred at 210 nm) with the lowest energy transitions located in the 320 –350 nm range [44–46]. No size effects are observed on the optical response of the powder; on the other hand, the surface functionalization through APTES condensation results in a red-shift of the low energy transitions, likely due to the increase of surface defects.

The absorption spectra of the silica suspensions are affected by light scattering effects (Fig. 3b) due to the colloidal nature of the particles, making the absorption spectra not sensitive enough to monitor the dye degradation, which is carried out by fluorescence techniques.

Acridine orange zinc chloride double salt is an orange fluorescent cationic dye, member of the heterocyclic acridine family (the structure is shown in Fig. 4). The absorption spectrum of the dye has two main transition bands: one with maxima at 268 and 288 nm and the other centred at 490 nm with a shoulder at 470 nm. This particular dye was chosen as its absorption profiles show minimal overlap with the electronic transitions of the semiconductor, thus allowing independent excitation of the NPs and the dye and enabling to acquire information about the irradiation wavelength effects on the degradation process. The fluorescence spectra collected upon excitation at 490 nm show a structureless emission band centred at 530 nm.

3.3. Degradation of AO aqueous solutions by SNP and SNP-APTES photocatalysts

The photoinduced degradation experiments are carried out using both silica NPs (SNP1 and SNP2) and aminopropyl-functionalized silica NPs (SNP1-APTES and SNP2-APTES) as

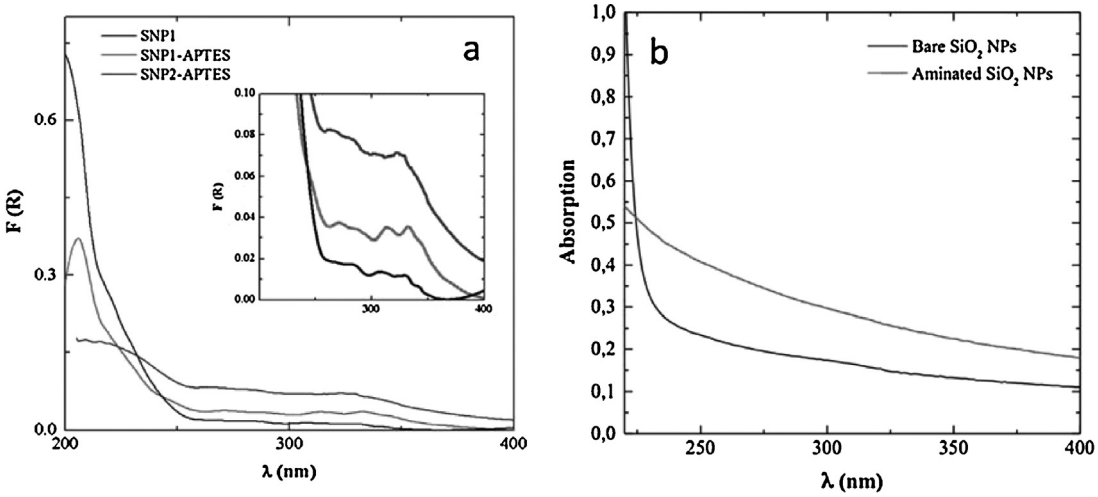

Fig. 3. UV–vis absorption spectra of SNP1 (black line), SNP1-APTES (red line) and SNP2-APTES (blue line) in powder form (a) and in aqueous suspensions (b). (For interpretation of the references to color in this figure legend, the reader is referred to the web version of this article.)

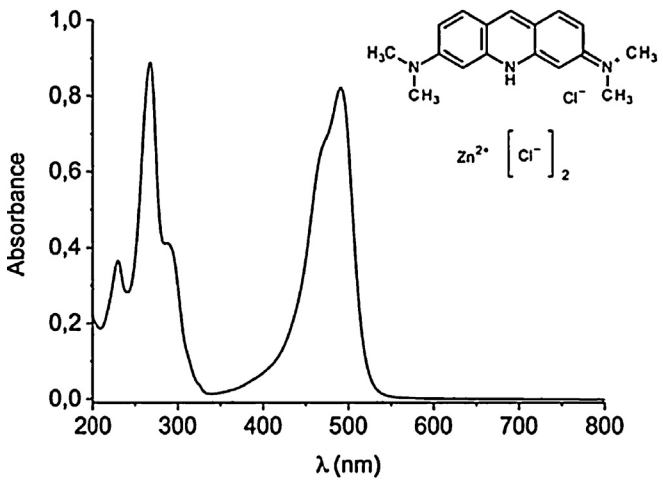

Fig. 4. Structure of acridine orange hemi (zinc chloride) salt and its absorption spectra in water.

catalysts. Irradiation at 313 and 490 nm is performed to determine the dye degradation efficiencies and to obtain information on the two different activation processes.

The effect of the irradiation on the dye concentration is investigated by monitoring the intensity of the dye fluorescence at 530 nm at different times. The decrease of the emission intensity is correlated to the decrease of the dye concentration, since no modifications of the spectral shape are observed (Figs. 5 and 6). The fluorescence intensity data at different irradiation times are used to determine the rate of dye degradation (Fig. 7).

Similar irradiation experiments are carried out on the dye solutions without silica NPs and they are used as reference experiments. In the absence of catalyst, no fluorescence decrease is detected indicating that the degradation efficiency of the dye is negligible in the absence of silica under the used experimental conditions.

We do not observe AO degradation under UV or vis light when the bare silica NPs (SNP1 and SNP2) are used. Instead, a significant dye decoloration efficiency is achieved (from 37 to 58%) with 3-aminopropyl-functionalized silica NPs upon irradiation at 313 or 490 nm for 50 minutes. Table 2 reports the photodegradation

Table 2
Parameters for the photodegradation of acridine orange in the presence of silica NPs.[a,b]

Catalyst	λ_{exc} (nm)	Photo degradation efficiency R (%)	k(min^{-1})	Half-time $t_{1/2}$(min)
SNP1	313	0	–	
SNP1	490	0	–	
SNP1-APTES	313	37	0.136	5
SNP1-APTES	490	58	0.018	38
SNP2	313	0	–	
SNP2	490	0	–	
SNP2-APTES	313	55	0.016	42
SNP2-APTES	490	58	0.015	46

[a] Dye concentration 1.0×10^{-5} M.
[b] Catalyst concentration 3.3 g/L.

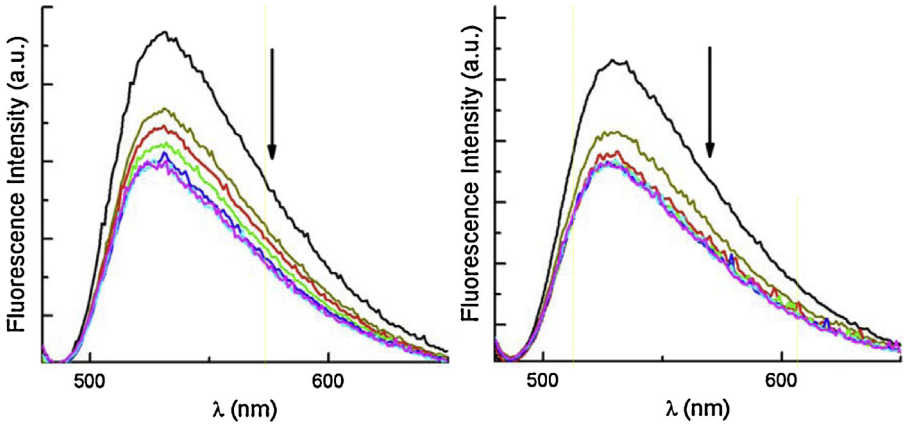

Fig. 5. Fluorescence spectra of AO recorded at different irradiation times (0–50 min) in the presence of SNP1-APTES (λ_{irr} = 490 nm, left panel and 313 nm, right panel).

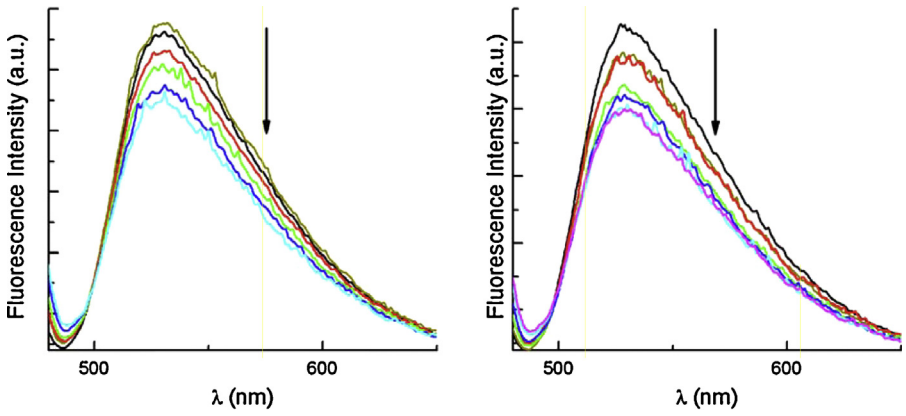

Fig. 6. Fluorescence spectra of AO recorded at different irradiation times (0–50 min) in the presence of SNP2-APTES (λ_{irr} = 490 nm, left panel and 313 nm, right panel).

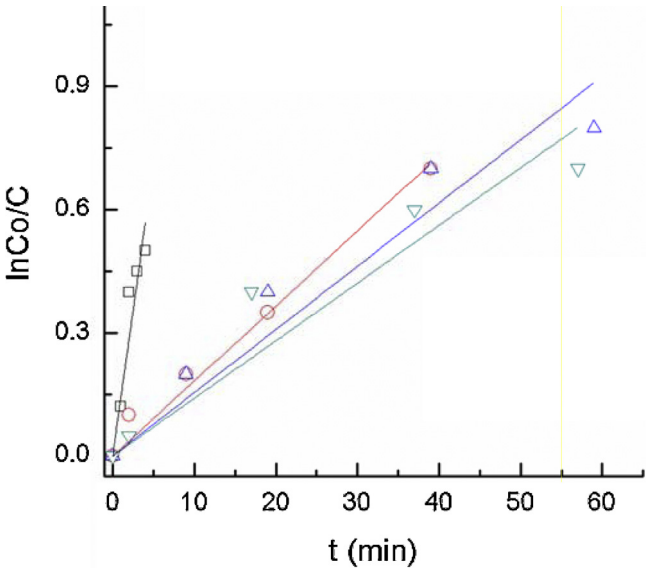

Fig. 7. Kinetic analysis of the photodegration data recorded in different experimetal conditions.

efficiencies of AO when irradiated at 313 and 490 nm in the presence of SNP1, SNP2, SNP1-APTES and SNP2-APTES, respectively. The observed absence of dye degradation without silica confirms the photocatalytic properties of the colloids. The catalysts obtained by functionalization of 55 nm NPs (SNP1-APTES) show a higher photocatalytic activity at 490 nm (58%) than at 313 nm (37%), whereas those obtained by functionalization of 146 nm NPs (SNP2-APTES) have similar efficiency at both excitation wavelengths (55% and 58%, respectively, Table 2).

3.4. Kinetic analysis of the fluorescence data

The analysis of the fluorescence data as function of the irradiation time gives information about the reaction rates of the photodegradation process.

The results of the photocatalytic experiments showed that the degradation of AO obeys to a pseudo-first order kinetic law, which can be expressed in the following form:

$$-\ln\left(\frac{C}{C_0}\right) = kt \quad (1)$$

where C is the concentration of dye at time t, C_0 the initial concentration of dye and k the pseudo first-order rate constant and t corresponds to the irradiation time. The half-life $t_{1/2}$ was determined according to Eq. (2):

$$t_{1/2} = 0.963k^{-1} \quad (2)$$

The reaction rate constants (k), obtained from the slope of the plots of $-\ln(C/C_0)$ versus t (Fig. 7) and the half-lifes $t_{1/2}$ are listed in Table 2. The k values are 0.136 and 0.016 min^{-1} for SNP1-APTES and SNP2-APTES, respectively under UV light and 0.018 and 0.015 min^{-1} for SNP1-APTES and SNP2-APTES, respectively under visible light. Consequently, $t_{1/2}$ is 5 and 42 min under UV light and 38 and 46 min under vis light for SNP1-APTES and SNP2-APTES, respectively.

4. Discussion

The presented data indicate that an efficient AO degradation occurs when amino-functionalized silica particles are used and the disappearance rates of the dye upon vis or UV irradiation are comparable.

The adsorption process in aqueous solution depends on the chemical properties of the adsorbent and the adsorbate, such as functional groups, surface charge, and hydrophilic and hydrophobic nature. In general, three types of interactions, through which the dye is adsorbed on silica nanobeads, can occur: electrostatic attraction, hydrophobic interaction and hydrogen bonding. SNP1 and SNP2 samples used in this study have silanol groups on the surface, which result in a net negative surface charge, as indicated by zeta-potential measurements; therefore an electrostatic attraction between the cationic dye and the silica surface is expected to drive the interaction. Instead, we do not observe degradation of the cationic dye, independently from the excitation wavelength. Several authors have demonstrated that the adsorption capacity of some organic dyes is much higher on organic hybrid silica phases than on pure silica suggesting that hydrophobic interactions between the surface organic groups of the hybrid silica and the organic dyes play an important role in the adsorption process [40,41,47,48]. Then, SNP1-APTES and SNP2-APTES were synthesized and tested as photocatalysts to activate the decoloration process.

The decrease of the emission intensity of AO observed after irradiation in the presence of SNP1-APTES and SNP2-APTES (Figs. 5 and 6) proved that the organo-functionalization of silica NPs improves the degradation efficiency of the catalyst. The higher catalytic activity observed with these functionalized samples, particularly with SPN2-APTES, can be attributed to the higher hydrophobicity, which increases the affinity and the adsorption capacity towards the organic dye.

Under vis irradiation, the light is absorbed by the dye; in the used experimental conditions AO is protonated and in monomeric form [49]. In basic conditions, it has been observed that the main deactivation paths of electronically excited AO are fluorescence and triplet state formation [50,51]; both singlet and triplet states can transfer electrons to acceptor species, similarly to what observed for molecules adsorbed on titania [19], and the electron transfer process can be even more efficient if basic AO is formed [52]. However, the adsorption of acridine dyes on oxide surfaces enhances the population of triplet states with strong charge transfer character [53]. The observation that only amine-modified NPs assist the photodegradation of the dye suggests that the particle functional groups either alter the protolytic equilibrium of AO or strengthen the affinity between the dye and the colloids leading to chemiadsorbed species.

The photodegradation process occurs with remarkable efficiencies also under UV irradiation (313 nm), where the light is mainly absorbed by the silica NPs, likely through the involvement of defect states, as suggested by the absorption spectra of bare and functionalized silica NPs. The presence of optically active defects on amorphous silica nanomaterials has been reported [54,55]. Upon light absorption, in the silica NPs, an electron is promoted from the valence band forming charge carrier species (electron–hole). These species can be responsible for the degradation of the dye molecules [35] either directly through electron transfer processes or through the formation of reactive oxygen species (OH• radicals and/or superoxide radical anion $O_2^{\bullet -}$).

In addition, the absence of photodegradation observed for SNP1 and SNP2 and the similar degradation efficiencies (55 and 58%) and reaction rate constants (0.016 and 0.015 min^{-1}) recorded for SNP2-APTES (average size of 146 nm) irradiated at 313 or 490 nm prove that the interactions between the dye and the silica surface have a fundamental role in both activation processes.

Since the photoactivity of semiconductors is highly dependent on the specific surface area (surface area per unit gram of silica) and surface-to-volume ratio, which increase dramatically as particle size decreases [49,50], we expected a better photodegradation efficiency for the 55 nm NPs. On the contrary, we observed a sim-

ilar photoactivity for SNP1-APTES and SNP2-APTES at 490 nm and a reduced photoactivity (37%) at 313 nm for SNP1-APTES as compared to SNP2-APTES. This behaviour can be related to the different absorption cross section of the particles and the structural or electronic defects present on the two different kind of colloids, since no dependence of the electronic behaviour is expected for silica colloids. However, a possible modification of surface properties in SNP1-APTES during the catalytic process cannot be excluded at this stage since this colloid has the highest degradation rate constant ($0.136\,min^{-1}$) despite the lower efficiency compared to SNP2-APTES.

5. Conclusions

The presented results show that aqueous solutions of acridine orange (AO) can be photodegraded on amino functionalized silica NPs under UV or vis light illumination.

Silica NPs having a diameter of 55 or 146 nm are prepared by sol–gel procedures and their surface modified with amino groups to investigate the effects of functional groups on the silica surface on the dye degradation. The photodegradation experiments were carried out irradiating at 313 or 490 nm for 50 minute the aqueous samples of dye containing silica colloids. The photocatalytic degradation of the dye was determined upon monitoring the decrease of its fluorescence intensity. The AO fluorescence intensity does not change when bare SiO_2 beads are used as catalysts, whereas a significant decoloration efficiency (up to 58%) is achieved with amino functionalized NPs, with a photodegradation rate constant value of $0.136\,min^{-1}$. The data collected from the degradation experiments and kinetic analysis demonstrate that the functional groups on the silica surface have a fundamental role in the rate of degradation processes. Further investigations are currently in progress to characterize the intermediate species and reach a full description of the photoinduced process from a mechanistic point of view.

The possibility to use a material with a low environmental impact as silica to degrade dye pollutants under solar irradiation might open a new approach for remediation of wastewaters.

Acknowledgements

The support of the University of Perugia is gratefully acknowledged. L.T. thanks the support of Regione Umbria under the framework POR-FSE 2007–2013.

References

[1] T. Kurbus, Y.M. Slokar, A.M. Le Marechal, D.B. Voncina, Dyes Pigm. 58 (2003) 171–178, No. 2.
[2] A. Reife, H.S. Fremann, Environmental Chemistry of Dyes and Pigments, Wiley, New York, 1996.
[3] A. Iagatti, R. Flamini, M. Nocchetti, L. Latterini, J. Phys. Chem. C 117 (2013) 23996–24002.
[4] F. Zhang, J. Zhao, T. Shen, H. Hidaka, E. Pelizzetti, N. Serpone, Appl. Catal. B 15 (1998) 147–156.
[5] M.J. Garcia-Martinez, I. Da Riva, L. Canoira, J.F. Llamas, R. Alcantara, J.L.R. Gallego, Appl. Catal. B 67 (2006) 279–289.
[6] T.L. Thompson, J.T. Yates Jr., Chem. Rev. 106 (2006) 4428–4453.
[7] J.M. Macak, M. Zlamal, J. Krysa, P. Schmuki, Small 3 (2007) 300–304, No. 2.
[8] C. Tian, Q. Zhang, A. Wu, M. Jiang, Z. Liang, B. Jiang, H. Fu, Chem. Commun. 48 (2012) 2858–2860.
[9] M. Schiavello, Photocatalysis and Environment: Trends and Applications, Kluwer Academic Publishers, Dordecht, 1988.
[10] N. Serpone, E. Pelizzetti, Photocatalysis Fundamentals and Applications, Wiley Interscience, New York, 1989.
[11] M.A. Fox, M.T. Dulay, Heterogeneous photocatalysis, Chem. Rev. 93 (1993) 341–357.
[12] C. Galindo, P. Jacques, A. Kalt, J. Photochem. Photobiol. A 141 (2001) 47–56.
[13] A.A. Khodja, T. Sehili, J.F. Pilichowski, P. Boule, J. Photochem. Photobiol. A 141 (2001) 231–239.
[14] C. Guillard, H. Lachheb, A. Honas, M. Ksibi, J.M. Hermann, J. Photochem. Photobiol. A 158 (2003) 27–36.
[15] S. Lathasree, R. Nageswara, B. Sivasankar, V. Sadasivam, K. Rengaraj, J. Mol. Catal. A 223 (2004) 101–105.
[16] E. Kusvuran, O.M. Atanur, O. Erbatur, Appl. Catal. B 58 (2005) 211–216.
[17] H. Hidaka, J. Zhao, E. Pelizzetti, N. Serpone, J. Phys. Chem. 96 (1992) 2226.
[18] M. Pelaez, N.T. Nolan, S.C. Pillai, M.K. Seery, P. Falaras, A.G. Kontos, P.S.M. Dunlop, J.W.J. Hamilton, J.A. Byrne, K. O'shea, M.H. Entezari, D.D. Dionysiou, Appl. Catal. B 125 (2012) 331–349.
[19] Y. Wang, H. Zhang, P. Liu, X. Yao, H. Zhao, RSC Adv. 3 (2013) 8777–8782.
[20] G. Sivalingam, K. Nagaveni, M.S. Hegde, G. Madras, Appl. Catal. B 45 (2003) 23–38.
[21] K. Vinod Gopal, P.V. Kamat, Envorn. Sci. Technol. 29 (1995) 841–845.
[22] B. Neppolian, H.C. Choi, S. Sakthivel, B. Arabindoo, V. Murugesan, J. Hazard. Mater. B 89 (2002) 303–317.
[23] C. Lizama, J. Freer, J. Baeza, H.D. Mansilla, Catal. Today 76 (2002) 235–246.
[24] N. Daneshvar, D. Salari, A.R. Khataee, J. Photochem. Photobiol. A 157 (2003) 111–116.
[25] A. Akyol, H.C. Yatmaz, M. Bayramoglu, Appl. Catal. B 54 (2004) 19–24.
[26] S.K. Kansal, M. Singh, D. Sud, J. Hazard. Mater. 141 (2007) 581–590.
[27] G. Alberto, I. Miletto, G. Viscardi, G. Caputo, L. Latterini, S. Coluccia, G. Martra, J. Phys. Chem. C 113 (2009) 21048–21053.
[28] L. Latterini, M. Amelia, Langmuir 25 (2009) 4767–4773.
[29] V. Ambrogi, L. Perioli, C. Pagano, L. Latterini, F. Marmottini, M. Ricci, C. Rossi, Microporous Mesoporous Mater. 147 (2011) 343–349.
[30] A. Ogata, A. Kazusaka, M. Enyo, J. Phys. Chem. 90 (1986) 5201–5205.
[31] H. Yoshida, K. Kimura, Y. Inaki, T. Hattori, Chem. Commun. (1997) 129–130.
[32] H. Yoshida, T. Tanaka, S. Matsuo, T. Funabiki, S. Yoshida, J. Chem. Soc. Chem. Commun. (1995) 761–762.
[33] Y. Inaki, H. Yoshida, K. Kimura, S. Inagaki, Y. Fukushima, T. Hattori, Phys. Chem. Chem. Phys. 2 (2000) 5293–5297.
[34] Y. Inaki, H. Yoshida, T. Yoshida, T. Hattori, J. Phys. Chem. B 106 (2002) 9098–9106.
[35] Y. Badr, M.A. Mahmoud, J. Phys. Chem. Solids 68 (2007) 413–419.
[36] L.L. Hench, J.K. West, Chem. Rev. 90 (1990) 33–72.
[37] S. Santra, P. Zhang, K. Wang, R. Tapec, V. Tan, Anal. Chem. 73 (2001) 4988–4993.
[38] W. Stober, A. Fink, E. Bohn, J. Colloid Interface Sci. 26 (1968) 62–69.
[39] M. Jafarzadeh, I. AbRahman, C.S. Sipau, Synth. Met. 162 (2012) 466–476.
[40] Z. Wu, H. Joo, I.-S. Ahn, S. Haam, J.-H. Kim, K. Lee, Chem. Eng. J. 102 (2004) 277–282.
[41] Z. Wu, H. Xiang, T. Kim, M.-S. Chun, K. Lee, J. Colloid Interface Sci. 304 (2006) 119–124.
[42] E. Papirer, Adsorption on silica surfaces Surfactant Science Series, vol. 90, CRC Press, New York, 2000.
[43] H. Kamiya, M. Mitsui, H. Takano, S. Miyazawa, J. Am. Ceram. Soc. 83 (2000) 287–293.
[44] I.A. Rahmana, P. Vejayakumarana, C.S. Sipauta, J. Ismaila, C.K. Cheeb, Mater. Chem. Phys. 114 (2009) 328–332.
[45] R. Stanleya, A. Samson Nesarajb, Int. J. Appl. Sci. Eng. 12 (2014) 9–21, No. 1.
[46] A. YelilArasi, M. Hema, P. Tamilselvi, R. Anbarasan, Indian J. Sci. 1 (2012) 6–10, No. 1.
[47] T. Jesionowsk, Colloids Surf. A 222 (2003) 87–94.
[48] A. Andrzejewska, A. Krysztafkiewicz, T. Jesionowski, Dyes Pigm. 75 (2007) 116–124.
[49] R.D. Falcone, N.M. Correa, M.A. Biasutti, J.J. Silber, Langmuir 18 (2002) 2039–2047.
[50] M.Z. Chan, J.R. Bolton, Photochem. Photobiol. 34 (1981) 537–547.
[51] A. Kellmann, Y. Lion, Photochem. Photobiol. 29 (1979) 217–222.
[52] W.D. Cook, S. Chen, F. Chen, M.U. Kahveci, Y. Yagci, J. Pol. Sci. A 47 (2009) 5474–5487.
[53] P.V. Kamat, Chem. Rev. 93 (1993) 207–300.
[54] A.M. Chizhik, A.I. Chizhik, R. Gutbrod, A.J. Meixner, T. Schmidt, J. Sommerfeld, F. Huisken, Nano Lett. 9 (2009) 3239–3244.
[55] L. Skuja, J. Non-Cryst. Solids 239 (1998) 16–48.